Symmetrized Characterization of Noisy Quantum Processes

Joseph Emerson, *et al.*

Science **317**, 1893 (2007);
DOI: 10.1126/science.1145699

Science (print ISSN 0036-8075; online ISSN 1095-9203) is published weekly, except the last week in December, by the American Association for the Advancement of Science, 1200 New York Avenue NW, Washington, DC 20005.

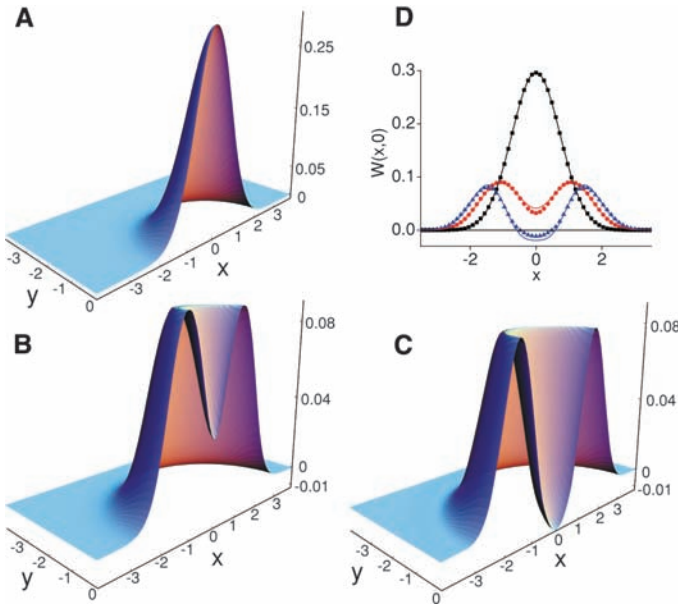

Fig. 4. Experimental WFs (corrected for detection inefficiency) for (**A**) the original thermal state; (**B**) the photon-added-then-subtracted state; (**C**) the photon-subtracted-then-added state. (**D**) presents sections of the above Wigner functions (black squares correspond to the thermal field; red circles and blue triangles correspond to the photon-added-then-subtracted and the photon-subtracted-then-added states, respectively), together with the corresponding theoretical predictions (solid curves) (*2*).

verse order, as in this case, is the real essence of the Heisenberg uncertainty principle. Besides its fundamental importance, the experimental implementation of such a sequence of basic quantum operations is an essential tool for the full-scale engineering of a quantum light state optimized for a multitude of different tasks (*15*), including robust quantum communication. As any quantum operation, including non-Gaussian operations, is composed of photon additions and subtractions (i.e, it can be expressed as $f(\hat{a},\hat{a}^{\dagger})$), our experimental results constitute a step toward the full quantum control of a field and the generation of highly entangled states (*16*).

References and Notes

1. P. A. M. Dirac, *The Principles of Quantum Mechanics* (Oxford Press, 1954).
2. Materials and methods are available as supporting material on *Science* Online.
3. A. Zavatta, S. Viciani, M. Bellini, *Science* **306**, 660 (2004).
4. A. Zavatta, S. Viciani, M. Bellini, *Phys. Rev. A* **72**, 023820 (2005).
5. A. Zavatta, V. Parigi, M. Bellini, *Phys. Rev. A* **75**, 052106 (2007).
6. C. T. Lee, *Phys. Rev. A* **52**, 3374 (1995).
7. J. Wenger, R. Tualle-Brouri, P. Grangier, *Phys. Rev. Lett.* **92**, 153601 (2004).
8. M. S. Kim, E. Park, P. L. Knight, H. Jeong, *Phys. Rev. A* **71**, 043805 (2005).
9. A. Zavatta, M. Bellini, P. L. Ramazza, F. Marin, F. T. Arecchi, *J. Opt. Soc. Am. B* **19**, 1189 (2002).
10. K. Banaszek, G. M. D'Ariano, M. G. A. Paris, M. F. Sacchi, *Phys. Rev. A* **61**, 010304(R) (1999).
11. A. I. Lvovsky, *J. Opt. B: Quantum Semiclassical Opt.* **6**, S556 (2004).
12. Z. Hradil, D. Mogilevtsev, J. Rehacek, *Phys. Rev. Lett.* **96**, 230401 (2006).
13. U. Leonhardt, *Measuring the Quantum State of Light* (Cambridge University Press, Cambridge, 1997).
14. Note that the positivity of the WF in the case of the add-then-subtract sequence is not due to experimental imperfections. As for squeezed states, the resulting state can be shown to be nonclassical (with a negative P function), although possessing a positive WF.
15. F. Dell'Anno, S. De Siena, F. Illuminati, *Phys. Rep.* **428**, 53 (2006).
16. J. Eisert, S. Scheel, M. B. Plenio, *Phys. Rev. Lett.* **89**, 137903 (2002).

17. We thank F. T. Arecchi, A. Montina, and E. Park for helpful comments and for a critical reading of the manuscript, and P. Poggi for the improvement of detection electronics. This work was partially supported by Ente Cassa di Risparmio di Firenze and by the Italian Ministry of University and Scientific Research, under the PRIN 2005 initiative. M.S.K. acknowledges financial support from the UK Engineering and Physical Science Research Council (EPSRC) and Quantum Information Processing Interdisciplinary Research Centre (QIPIRC).

Supporting Online Material

www.sciencemag.org/cgi/content/full/317/5846/1890/DC1
Materials and Methods
References and Notes

7 June 2007; accepted 10 August 2007
10.1126/science.1146204

Symmetrized Characterization of Noisy Quantum Processes

Joseph Emerson,[1,2] Marcus Silva,[2,3] Osama Moussa,[2,3] Colm Ryan,[2,3] Martin Laforest,[2,3] Jonathan Baugh,[2] David G. Cory,[4] Raymond Laflamme[2,3,5]

A major goal of developing high-precision control of many-body quantum systems is to realize their potential as quantum computers. A substantial obstacle to this is the extreme fragility of quantum systems to "decoherence" from environmental noise and other control limitations. Although quantum computation is possible if the noise affecting the quantum system satisfies certain conditions, existing methods for noise characterization are intractable for present multibody systems. We introduce a technique based on symmetrization that enables direct experimental measurement of some key properties of the decoherence affecting a quantum system. Our method reduces the number of experiments required from exponential to polynomial in the number of subsystems. The technique is demonstrated for the optimization of control over nuclear spins in the solid state.

Quantum information enables efficient solutions to certain tasks that have no known efficient solution in the classical world, and it has reshaped our understanding of computational complexity. Harnessing the advantages of the quantum world requires the ability to robustly control quantum systems and, in particular, counteract the noise and decoherence affecting any physical realization of quantum information processors (QIPs). A pivotal step in this direction came with the discovery of quantum error correction codes (QECCs) (*1*, *2*) and the threshold theorem for fault-tolerant (FT) quantum computation (*3*–*6*). To make use of quantum error correction and produce fault-tolerant protocols, we need to understand the nature of the noise affecting the system at hand. There is a direct way to fully characterize the noise using a procedure known as process tomography (*7*–*9*). However, this procedure requires resources that grow exponentially with the number of subsystems (usually two-level systems called "qubits") and is intractable for characterizing the multi-qubit quantum systems that are presently realized

[1]Department of Applied Math, University of Waterloo, Waterloo, ON N2L 3G1, Canada. [2]Institute for Quantum Computing, University of Waterloo, Waterloo, ON N2L 3G1, Canada. [3]Department of Physics and Astronomy, University of Waterloo, Waterloo, ON N2L 3G1, Canada. [4]Department of Nuclear Science and Engineering, Massachusetts Institute of Technology, Cambridge, MA 02139, USA. [5]Perimeter Institute for Theoretical Physics, Waterloo, ON N2L 2Y5, Canada.

(*10*–*12*). We introduce a general symmetrization method that allows for direct experimental characterization of some physically relevant features of the decoherence and apply it to develop an efficient experimental protocol for measuring multiqubit correlations and memory effects in the noise. Compared with existing methods (*13*), the protocol yields an exponential savings in the number of experiments required to obtain such information. In the context of applications, this information enables optimization of error-correction strategy and tests of some assumptions underlying estimates of the FT threshold. Moreover, the estimated parameters are immediately relevant for optimizing experimental control methods.

Focusing on a system of n qubits, a complete description of a general noise model Λ requires $O(2^{4n})$ parameters. Clearly an appropriate coarse-graining of this information is required; the challenge is to identify efficient methods for estimating the features of practical interest. The method we propose is based on identifying a symmetry associated with a property of interest, and then operationally symmetrizing the noise to yield an effective map $\overline{\Lambda}$, with a reduced number of independent parameters reflecting these properties (Fig. 1). This symmetrization is achieved by conjugating the noise (Fig. 2) with a unitary operator drawn randomly from the relevant symmetry group and then averaging over these random trials (*14*–*18*). We show below that rigorous statistical bounds guarantee that the number of experimental trials required is independent of the dimension of the group. Hence, our randomization method leads to efficient partial characterization of the map Λ whenever the group elements admit efficient circuit decompositions.

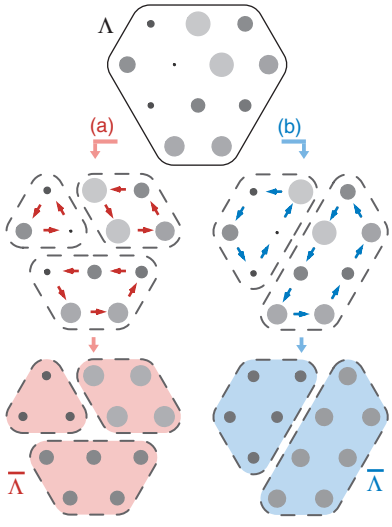

Fig. 1. Schematic of coarse-graining by symmetrization. Averaging the noise Λ by twirling under a symmetry group yields an effective noise process that has a reduced number of independent parameters. Distinct symmetrization groups [represented by (a) red and (b) blue] uniformize different subsets of parameters.

We apply this general idea to the important problem of estimating the noise parameters that determine the performance of a broad class of QECCs and the applicability of certain assumptions underlying FT thresholds. In general, QECCs protect quantum information only against certain types of noise. A distance-$(2t + 1)$ code refers to codes that correct all errors simultaneously, affecting up to t qubits. Hence, the distance of a QECC determines which terms in the noise will be corrected and which will remain uncorrected. The latter contribute to the overall failure probability. To estimate the failure probability, many fault-tolerance theorems assume that the noise is independent from qubit to qubit or between blocks of qubits. Another common assumption is that the noise is memoryless and hence Markovian in time. Our protocol enables measurements of these noise correlations under a given experimental arrangement without the exponential overhead of process tomography. This protocol is efficient also in the context of an ensemble QIP with highly mixed states (*19*).

We start by expanding the noise operators in the basis $P_i \in P_n$, consisting of n-fold tensor product of the usual single-qubit Pauli operators $\{1, X, Y, Z\}$ satisfying the orthogonality relation $\mathrm{Tr}[P_i\ P_j] = 2^n\ \delta_{ij}$. The Clifford group $\mathcal{C}_n$ is defined as the normalizer of the Pauli group $\mathcal{P}_n$: it consists of all elements U_i of the unitary group $U(2^n)$ satisfying $U_i P_j U_i^\dagger \in \mathcal{P}_n$ for every $P_j \in \mathcal{P}_n$. The protocol requires symmetrizing the channel $\Lambda \rightarrow \overline{\Lambda}$ by averaging over trials in which the channel is conjugated by the elements of $\mathcal{C}_1$ applied independently to each qubit (Fig. 2). An average over conjugations is known as a "twirl" (*20*), and we call the above a $\mathcal{C}_1^{\otimes n}$-twirl.

Separating out terms according to their Pauli weight w, where $w \in \{0,...,n\}$ is the number of nonidentity factors in P_l, letting the index $\nu_w \in \{1, ..., \binom{n}{w}\}$ count the number of distinct ways that w nonidentity Pauli operators can be distributed over the n factor spaces, and the index $\mathbf{i}_w = \{i_1, ..., i_w\}$ with $i_j \in \{1, 2, 3\}$ denote which of the nonidentity Pauli operators occupies the j^{th} occupied site, we obtain (see SOM text)

$$\overline{\Lambda(\rho)} = \sum_{w=0}^{n} \sum_{\nu_w=1}^{\binom{n}{w}} r_{w,\nu_w} \sum_{\mathbf{i}_w} P_{w,\nu_w,\mathbf{i}_w} \rho P_{w,\nu_w,\mathbf{i}_w} \quad (1)$$

where the reduced parameters $r_{w,\nu w}$ are fixed by Λ and $p_w = 3^w \sum_{\nu_w=1}^{\binom{n}{w}} r_{w,\nu w}$ are the probabilities of w simultaneous qubit errors in the noise. Some intuition about how a $\mathcal{C}_1^{\otimes n}$-twirl simplifies the task of noise characterization is obtained by analyzing the case of a single qubit (SOM text).

To measure these probabilities, we probe $\overline{\Lambda}$ with input state $|0\rangle \equiv |\ 0\rangle^{\otimes n}$, followed by a projective measurement of the output state in the basis $|l\rangle$. This yields an n-bit string $l \in \{0, 1\}^n$. Let q_w denote the probability that a random subset of w bits of the binary string l has even parity. This gives the eigenvalues of $\overline{\Lambda}$ as $c_w \equiv \langle \overline{Z^{\otimes w}} \rangle = 2q_w - 1$, and we obtain $p_{w'} = \sum_w \Omega^{-1}_{w',w} c_w$,

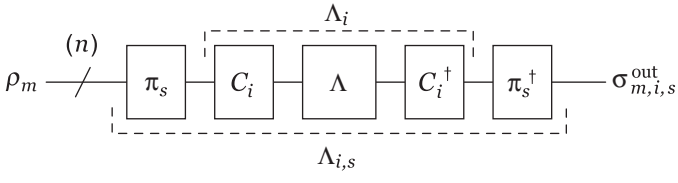

Fig. 2. Quantum circuit. One experimental run consists of a conjugation of the noise process Λ. The standard protocol requires conjugation only by an element C_i, whereas the ensemble protocol requires conjugating Λ also by a permutation π_s of the qubits. The standard protocol requires only one input state $|\ 0\rangle^{\otimes n}$, whereas the ensemble protocol requires n distinct input operators ρ_w.

Table 1. Summary of experimental results. The first four sets of experiments (three sets on the two-qubit liquid-state system and one on the three-qubit solid-state system) were designed to characterize the performance of the protocol under engineered noise. The final two sets demonstrate characterization of the (unknown) natural noise affecting the quantum memory created by multiple-pulse time-suspension sequences with different pulse spacings.

No.	System	Map description	Kraus operators (A_k)	k	p_0	p_1	p_2	p_3
1	$CHCl_3$	Engineered: $\mathbf{p} = [0,1,0]$.	$\frac{1}{\sqrt{2}}\{Z_1, Z_2\}$	288	$0.000^{+0.004}$	$0.991^{+0.009}_{-0.015}$	$0.009^{+0.017}_{-0.009}$	-
2	$CHCl_3$	Engineered: $\mathbf{p} = [0,0,1]$.	$\{Z_1\ Z_2\}$	288	$0.001^{+0.006}_{-0.001}$	$0.004^{+0.011}_{-0.004}$	$0.996^{+0.004}_{-0.011}$	-
3	$CHCl_3$	Engineered: $\mathbf{p} = [\frac{1}{4}, \frac{1}{2}, \frac{1}{4}]$.	$\{\exp[i\frac{\pi}{4}(Z_1 + Z_2)]\}$	288	$0.254^{+0.010}_{-0.010}$	$0.495^{+0.021}_{-0.020}$	$0.250^{+0.019}_{-0.019}$	-
4	$C_3H_4O_4$	Engineered: $\mathbf{p} = [0,1,0,0]$.	$\frac{1}{\sqrt{3}}\{Z_1, Z_2, Z_3\}$	432	$0.01^{+0.01}_{-0.01}$	$0.99^{+0.01}_{-0.03}$	$0.01^{+0.02}_{-0.01}$	$0.00^{+0.01}$
5	$C_3H_4O_4$	Natural Noise (i)	unknown	432	$0.44^{+0.01}_{-0.02}$	$0.45^{+0.03}_{-0.03}$	$0.10^{+0.04}_{-0.08}$	$0.01^{+0.03}_{-0.01}$
6	$C_3H_4O_4$	Natural Noise (ii)	unknown	432	$0.84^{+0.01}_{-0.01}$	$0.15^{+0.02}_{-0.03}$	$0.01^{+0.03}_{-0.01}$	$0.00^{+0.02}$

where the matrix $\Omega^{-1}_{w',w}$ is a matrix of combinatorial factors (SOM text). If in each single-shot experiment, the Clifford operators are chosen uniformly at random, then with $K = O[\log(2n)/\delta^2]$ experiments we can estimate each of the coefficients c_w to precision δ with constant probability. All imperfections in the protocol contribute to the total probabilities of error. The protocol can be made robust against imperfections in the input state preparation, measurement, and twirling by factoring out the values $c_w(0)$ measured when the protocol is performed without the noisy channel: $c_w \rightarrow \tilde{c}_w = c_w/c_w(0)$.

The c_w can be applied directly to test some of the assumptions that affect estimates of the fault-tolerance threshold (*21*, *22*). In particular, a noisy channel with an uncorrelated distribution of error locations, but with arbitrary correlations in the error type, is mapped under our symmetrization to a channel that is a tensor product of n single-qubit depolarizing channels. A channel satisfying this property will exhibit the scaling $c_w = c_1^w$. Hence, observed deviations from this scaling imply a violation of the above assumption. However, there are correlated error models that also give rise to this scaling, so the converse implication does not hold.

Furthermore, we can test for non-Markovian properties by repeating the above scheme for distinct time intervals $m\tau$ with increasing m. If, over the time scale τ, the noise satisfies the Markovian semigroup property $\Lambda_\tau \circ \Lambda_\tau = \Lambda_{2\tau}$ (*23*), then so will the twirled map $\overline{\Lambda}_\tau \circ \overline{\Lambda}_\tau = \overline{\Lambda}_{2\tau}$. Consequently, the coefficients $c_w(m\tau)$ measured over the time-scale $m\tau$ will satisfy $c_w(m\tau) = c_w(\tau)^m$. Observed deviations from this scaling imply non-Markovian effects in the untwirled noise. However, again the converse does not hold; consistency with this scaling does not guarantee that the untwirled noise obeys the Markovian semigroup property.

When applying $\{c_w\}$ to estimate $\{p_w\}$, the statistical uncertainty for p_w grows exponentially with w (SOM text). This still allows for characterization of other important features of the noise. Specifically, the probability p_0 is directly related to the entanglement fidelity of the channel, so this protocol provides an exponential savings over recently proposed methods for estimating this single figure of merit (*16*, *24*, *25*). [For another approach, see (*17*)]. Hence, by actually implementing any given code, we can bound the failure probability of that code with only $O[\log(2n)/\delta^2]$ experiments and without making any theoretical assumptions about the noise. Moreover, on physical grounds, we may expect the noise to become independent between qubits outside some fixed (but unknown) scale b, after which the p_w decreases exponentially with w. The scale b can be determined efficiently with $O(n^b)$ experiments.

Although a characterization of the twirled channel is useful given the relevance of twirled channels in some fault-tolerant protocols (*22*), the failure probability of the twirled channel gives an upper bound to the failure probability of the original untwirled channel whenever the performance of the code has some bound that is invariant under the symmetry associated with the twirl. This holds quite generally in the context of the symmetry considered above because the failure probability of a generic distance-$(2t + 1)$ code is bounded above by the total probability of error terms with Pauli weight greater than t, and this weight remains invariant under conjugation by any $C_i \in \mathcal{C}_1^{\otimes n}$.

Our protocol is efficient also in the context of an ensemble QIP (*19*). We prepare deviations from the identity state of the form $\rho_w = Z^{\otimes w} \otimes 1^{\otimes(n-w)}$, with $w \in \{1, \ldots n\}$; hence, the (non-scalable) preparation of pseudo-pure states is avoided. As illustrated in Fig. 2, the ensemble protocol consists of conjugating the process $\Lambda \rightarrow \Lambda_{i,s}$ with a randomly chosen pair (C_i, π_s) in each run, where π_s is a random permutation of the qubits. For input operator ρ_w, the output is $\sigma^{out}_{w,i,s} = \Lambda_{i,s}(\rho_w)$. Averaging the output operators $\sigma^{out}_{w,i,s}$ over i and s returns the input operator scaled by c_w.

We performed an implementation of the above protocol on both a two-qubit (chloroform $CHCl_3$) liquid-state and a three-qubit (single-crystal Malonic acid $C_3H_4O_4$) solid-state nuclear magnetic resonance QIP (*26*). The results of these experiments are summarized in Table 1. Statistical analysis for one liquid-state set is shown in fig. S1 and for the final two solid-state sets in Fig. 3. The final two sets of (solid-state) experiments were performed to characterize the unknown residual noise occurring under (i) one cycle of a C48 pulse sequence (*27*) with 10 μs pulse spacing, and (ii) two cycles of C48 with 5 μs pulse spacing. The C48 sequence is designed to suppress the dynamics due to the system's internal Hamiltonian and could be used, for example, for quantum memory. The evolution of the system under this pulse sequence can be evaluated theoretically by calculating the Magnus expansion (*28*) of the associated effective Hamiltonian, under which the residual effects appear as a sum of terms associated with the Zeeman and dipolar parts of the Hamiltonian, including cross terms. Roughly speaking, effective suppression of the k^{th} term of the Hamiltonian takes places when $\gamma_k \tau_k << 1$, where γ_k is the strength of the term and τ_k^{-1} is the rate at which it is modulated by the pulse sequence. Generally, shorter delays lead to improved performance unless there is a competing process at the shorter time scale. Although two repetitions of the sequence with the pulse spacing of 5 μs has twice as many pulses as the single sequence with the 10 μs spacing, the probabilities of one-, two-, and three-body noise terms all decrease substantially (Table 1). However, the averaging under the 5 μs falls short of ideal performance as a result of incomplete (heteronuclear) decoupling of the qubits (three carbon nuclei) from the envi-

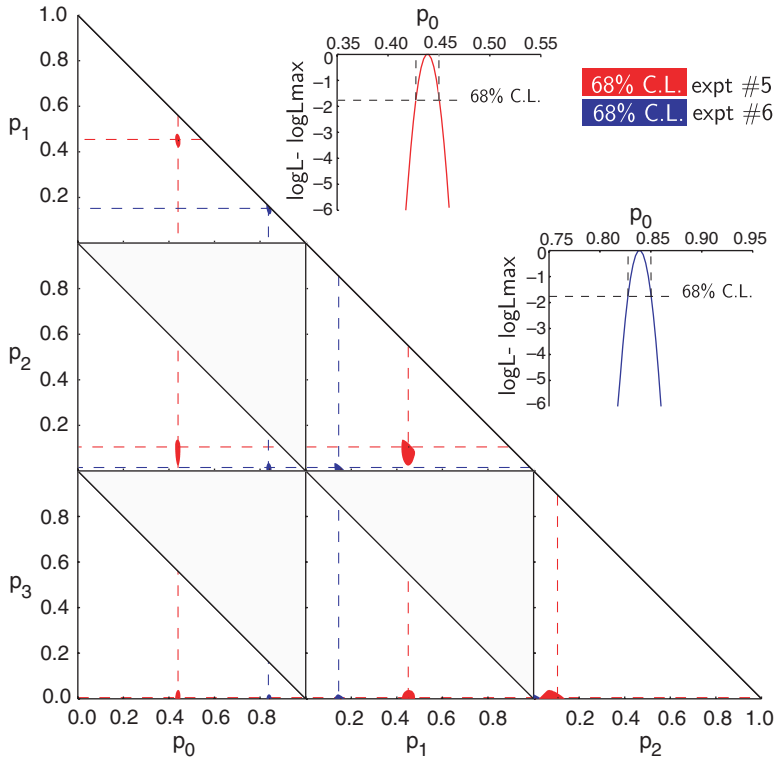

Fig. 3. Results for p_w from experiments 5 and 6 in Table 1. Shown are projections of the four-dimensional likelihood function onto various probability planes. The asymmetry seen in some of the confidence areas is a result of this projection. The results for one cycle with 10 μs pulse spacing (experiment 5) are in red, and the results for two cycles with 5 μs spacing (experiment 6) are in blue.

ronment (nearby hydrogen nuclei) (SOM text). For both sequences, the noise coefficients c_w do not statistically deviate from the scaling implied by uncorrelated errors (fig. S3), although, as noted above, this does not guarantee that the errors are uncorrelated.

Our method provides an efficient protocol for the characterization of noise in contexts where the target transformation is the identity operator, for example, a quantum communication channel or quantum memory. However, the protocol also provides an efficient means for characterizing the noise under the action of a nonidentity unitary transformation. One approach is to decompose the unitary transformation into a product of basic quantum gates drawn from a universal gate set, where each gate in the set acts on at most 2 qubits simultaneously. Hence, the noise map acting on all n qubits associated with any two-qubit gate can be determined by applying the above protocol to other $n-2$ qubits while applying process tomography to the two qubits in the quantum gate. Another approach is to estimate the average error per gate for a sequence of m gates, such that the composition gives the identity operator. Such a sequence can be generated by making use of the cyclic property $U^m = 1$ of any gate in a universal gate set or by choosing a sequence of $m-1$ random gates followed by an m^{th} gate chosen such that the composition gives the identity transformation.

References and Notes

1. P. W. Shor, *Phys. Rev. A* **52**, R2493 (1995).
2. A. M. Steane, *Phys. Rev. Lett.* **77**, 793 (1996).
3. P. W. Shor, *Proceedings of the Symposium on the Foundations of Computer Science,* 56 (IEEE press, Los Alamitos, California, 1996).
4. D. Aharonov, M. Ben-Or, *Proceedings of the 29th Annual ACM Symposium on the Theory of Computing,* 176 (ACM Press, New York, 1996).
5. A. Y. Kitaev, *Uspekhi Mat. Nauk.* **52**, 53 (1997).
6. E. Knill, R. Laflamme, W. Zurek, *Science* **279**, 342 (1998).
7. I. Chuang, M. Nielsen, *J. Mod. Opt.* **44**, 2455 (1997).
8. G. M. D'Ariano, P. Lo Presti, *Phys. Rev. Lett.* **86**, 4195 (2001).
9. M. Mohseni, D. Lidar, *Phys. Rev. Lett.* **97**, 170501 (2006).
10. H. Haffner *et al.*, *Nature* **438**, 643 (2005).
11. D. Leibfried *et al.*, *Nature* **438**, 639 (2005).
12. C. Negrevergne *et al.*, *Phys. Rev. Lett.* **96**, 170501 (2006).
13. A. Childs, I. Chuang, D. Leung, *Phys. Rev. A* **64**, 012314 (2001).
14. J. Emerson, Y. Weinstein, M. Saraceno, S. Lloyd, D. Cory, *Science* **302**, 2098 (2003).
15. B. Levi, C. Lopez, J. Emerson, D. G. Cory, *Phys. Rev. A* **75**, 022314 (2007).
16. J. Emerson, R. Alicki, K. Zyczkowski, *J. Opt. B: Quantum and Semiclassical Optics* **7**, S347 (2005).
17. C. Dankert, R. Cleve, J. Emerson, E. Livine, quant-ph/0606161 (2006).
18. W. Dur, M. Hein, J. Cirac, H.-J. Briegel, *Phys. Rev. A* **72**, 052326 (2005).
19. D. G. Cory *et al.*, *Fortschr. Phys.* **48**, 875 (2000).
20. C. Bennett, D. DiVincenzo, J. Smolin, W. Wootters, *Phys. Rev. A* **54**, 3824 (1996).
21. P. Aliferis, D. Gottesman, J. Preskill, *Quant. Inf. Comp* **6**, 97 (2006).
22. E. Knill, *Nature* **434**, 39 (2005).
23. R. Alicki, K. Lendi, *Quantum Dynamical Semigroups and Applications*, Lecture Notes in Physics **286**, 12 (1987).
24. E. Fortunato *et al.*, *J. Chem. Phys.* **116**, 7599 (2002).
25. M. Nielson, *Phys. Lett. A* **303**, 249 (2002).
26. Materials and methods are available as supporting material on *Science* Online.
27. D. G. Cory, J. B. Miller, A. N. Garroway, *J. Magn. Reson.* **90**, 205 (1990).
28. U. Haeberlen, *Advances in Magnetic Resonance*, Ed. J. Waugh, Academic Press, New York (1976).

29. This work benefited from discussions with R. Blume-Kohout, R. Cleve, M. Ditty, D. Gottesman, E. Knill, B. Levi, and A. Nayak and was supported by the National Science and Engineering Research Council of Canada (NSERC) grants 250673 and 327778, Ontario Research Development Challenge Fund (ORDCF) grant 3232301-05, Army Research Office/Laboratory for Physical Sciences (ARO/LPS) grant W911NF-05-1-0469, and Army Research Office/Mathematics of Information Technology and Complex Systems (ARO/MITACS) grant W911NF-05-1-0298.

Supporting Online Material

www.sciencemag.org/cgi/content/full/317/5846/1893/DC1
Materials and Methods
SOM Text
Figs. S1 to S3
References

25 May 2007; accepted 29 August 2007
10.1126/science.1145699

Nuclei-Induced Frequency Focusing of Electron Spin Coherence

A. Greilich,[1]* A. Shabaev,[2,3]* D. R. Yakovlev,[1,4] Al. L. Efros,[2]† I. A. Yugova,[1,5] D. Reuter,[6] A. D. Wieck,[6] M. Bayer[1]†

The hyperfine interaction of an electron with the nuclei is considered as the primary obstacle to coherent control of the electron spin in semiconductor quantum dots. We show, however, that the nuclei in singly charged quantum dots act constructively by focusing the electron spin precession about a magnetic field into well-defined modes synchronized with a laser pulse protocol. In a dot with a synchronized electron, the light-stimulated fluctuations of the hyperfine nuclear field acting on the electron are suppressed. The information about electron spin precession is imprinted in the nuclei and thereby can be stored for tens of minutes in darkness. The frequency focusing drives an electron spin ensemble into dephasing-free subspaces with the potential to realize single frequency precession of the entire ensemble.

The possibility of encoding quantum information in the spins of quantum dot (QD) electrons has attracted considerable attention (*1*, *2*). The spatial confinement protects the spins against the primary relaxation mechanisms in bulk, all of which arise from coupling of spin and orbital momenta. However, the electron hyperfine interaction with the lattice nuclei is enhanced by confinement, leading to spin decoherence and dephasing (*3*–*10*) and thus posing severe difficulties for processing quantum information. General schemes for suppressing decoherence have been discussed already (*11*). Electron spin relaxation in QDs may be overcome by polarizing the nuclear spins (*12*, *13*), but the high degree of polarization required, close to 100% (*12*), has not been achieved yet (*14*–*16*).

We find that the hyperfine interaction, rather than being detrimental, can be used as a precision tool by demonstrating that it modifies the continuous mode spectrum of the electron spin precession in a QD ensemble into a few discrete modes. The information on this digital spectrum can be stored in the nuclear spin system for tens of minutes because of the long nuclear memory times (*17*, *18*).

In a QD ensemble, fast electron spin dephasing arises not only from nuclear field fluctuations but also from variations of the electron g factor, leading to different spin precession frequencies. The dephasing due to these unavoidable variations can be partly overcome by mode-locking (*19*), which synchronizes the precession of specific electron spin modes in the ensemble with the clocking rate of a periodic pulsed laser. Still, it leaves a substantial fraction of dephased electron spins, whose precession frequencies do not satisfy the mode locking conditions. We demonstrate that the nuclear spin polarization adjusts the electron spin precession frequency in each quantum dot such that the whole ensemble becomes locked on very few frequencies.

The experiments were done on an ensemble of self-assembled (In,Ga)As/GaAs QDs (*19*, *20*), each dot containing on average a single electron (*21*). The electron spin precession about a perpendicular magnetic field was studied by a pump-probe Faraday rotation (FR) technique with ps time resolution (*22*). Spin coherence is generated

[1]Experimentelle Physik II, Universität Dortmund, D-44221 Dortmund, Germany. [2]Naval Research Laboratory, Washington, DC 20375, USA. [3]School of Computational Sciences, George Mason University, Fairfax, VA 22030, USA. [4]A. F. Ioffe Physico-Technical Institute, 194021 St. Petersburg, Russia. [5]Institute of Physics, St. Petersburg State University, 1908504 St. Petersburg, Russia. [6]Angewandte Festkörperphysik, Ruhr-Universität Bochum, D-44780 Bochum, Germany.

*These authors contributed equally to this work.
†To whom correspondence should be addressed. E-mail: efros@dave.nrl.navy.mil; manfred.bayer@physik.uni-dortmund.de

Supporting Online Material for

Symmetrized Characterization of Noisy Quantum Processes

Joseph Emerson, Marcus Silva, Osama Moussa, Colm Ryan,
Martin Laforest, Jonathan Baugh, David G. Cory, Raymond Laflamme

Published 28 September 2007, *Science* **317**, 1893 (2007)
DOI: 10.1126/science.1145699

This PDF file includes:

Symmetrised Characterisation of Noisy Quantum Processes

Joseph Emerson,[1,2] Marcus Silva,[3,2] Osama Moussa,[3,2] Colm Ryan,[3,2] Martin Laforest,[3,2] Jonathan Baugh,[2] David G. Cory,[4] and Raymond Laflamme[3,2]

[1]*Department of Applied Mathematics, University of Waterloo, Waterloo, ON N2L 3G1, Canada*
[2]*Institute for Quantum Computing, University of Waterloo, Waterloo, ON N2L 3G1, Canada*
[3]*Department of Physics and Astronomy, University of Waterloo, Waterloo, ON N2L 3G1, Canada*
[4]*Department of Nuclear Science and Engineering, Massachusetts Institute of Technology, Cambridge, MA 02139, USA*

Supporting Online Material

Materials and Methods

The two-qubit liquid-state experiments were performed on a sample made from 10mg of ^{13}C labeled chloroform (Cambridge Isotopes) dissolved in 0.51ml of deuterated acetone. The experiment was performed on a 700MHz Bruker Avance spectrometer using a dual inverse cryoprobe. The pulse programs were optimized on a home-built pulse sequence compiler which pre-simulates the pulses in an efficient pairwise manner and takes into account first order phase and coupling errors during a pulse by modifications of the refocussing scheme and pulse phases [1]. The solid-state experiments were performed on a single crystal of malonic acid which contained ≈7% triply labeled ^{13}C molecules [2]. The experiments were performed at room temperature with a home-built probe. Apart from an initial polarization transfer, the protons were decoupled using the SPINAL64 sequence [3]. The required control fields that implemented the unitary propagators and state-to-state transformations were found using the GRAPE optimal control method [4] and made robust to inhomogeneities in both the r.f. and static fields. The implemented versions of the pulses were corrected for non-linearities in the signal generation and amplification process through a pickup coil to measure the r.f. field at the sample and a simple feedback loop.

The error probabilities for each experiment were calculated using a constrained maximum likelihood function. The results of this analysis for one of the liquid-state experiments are shown in Fig. S1.

Supporting Text

Effect of Clifford Twirling on a Single Qubit

We can give some intuitive idea of how twirling leads to a reduction of the number of independent parameters by considering the case of a noisy channel for a single qubit. To demonstrate the main idea most directly, we consider a simple stochastic noise model of the form

$$\Lambda(\rho) = p_o 1\rho 1 + p_x X\rho X + p_y Y\rho Y + p_z Z\rho Z$$

which has three independent parameters (where $p_o + p_x + p_y + p_z = 1$). Under conjugation, the Clifford operators map each non-identity Pauli operator to another Pauli operator [5]. For example, conjugation of the Pauli operators under the Hadamard gate H, which is an element of the Clifford group, has the following effect: $HXH^\dagger = HXH = Z$, $HYH = -Y$, and $HZH = X$. Hence the H-conjugated noise model takes the form

$$H\Lambda(H\rho H)H = p_o 1\rho 1 + p_x Z\rho Z + p_y Y\rho Y + p_z X\rho X.$$

More generally, the 12 elements of the Clifford group for a single qubit divide into subsets of operators, where the elements of each subset map each non-identity Pauli to one of the three possible non-identity Pauli's. By averaging over each possible conjugation (operationally defined by the circuit given in Fig. 2), each of the possible Pauli errors becomes equiprobable, and the noise model transforms to the twirled form

$$\Lambda(\rho) \to \overline{\Lambda}(\rho) = p_o\rho + (p_1/3)(X\rho X + Y\rho Y + Z\rho Z),$$

where $p_1 = p_x + p_y + p_z$. As a result, we only need to estimate the probability of any one Pauli error in the twirled channel, and from that we can estimate the total probability of all 3 distinct single qubit Pauli errors in the un-twirled channel. The general analysis of a $\mathcal{C}_1^{\otimes n}$-twirl is described in detail below.

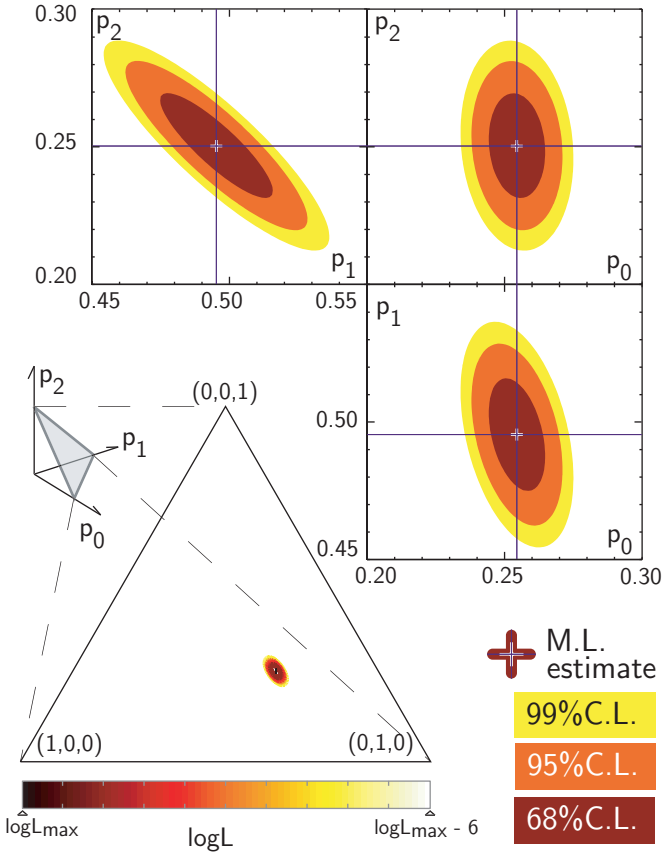

FIG. 1: **Results for Experiment #3 in Table 1.** Shown is the Maximum Likelihood (ML) estimate, $\mathbf{p}_{exp} = [0.254^{+0.010}_{-0.010}, 0.495^{+0.021}_{-0.020}, 0.250^{+0.019}_{-0.019}]$, for the error probabilities of the engineered noise, $A_1 = \{\exp[-i\pi(Z_1 + Z_2)/4]\}$, for which the calculated values are $\mathbf{p} = [1/4, 1/2, 1/4]$. Also shown are the confidence regions for the 68%, 95%, and 99% confidence levels (C.L.), which can be determined from the log of a likelihood function, $\log L$. The experiment was performed on a 2-qubit liquid-state NMR processor, and the noise was implemented by appropriately phase-shifting the pulses. These experiments illustrate the precision with which the protocol can be implemented under conditions of well-developed quantum control.

The other main ingredient of our analysis is the use of statistical bounds to prove that the set of all possible conjugations (which is exponentially large in the number of qubits) need not be performed to estimate the average. Specifically, the set of conjugations needs to be sampled a number of times that grows only logarithmically with the number of qubits. The details of this statistical analysis are provided further below.

General Analysis of the Symmetrisation

More generally, the generic noise affecting a quantum state ρ (a positive matrix of dimension $D \times D$) can be represented by a completely positive map of the form $\Lambda(\rho) = \sum_{k=1}^{D^2} A_k \rho A_k^\dagger$, which is normally subject to a trace-preserving condition $\sum_k A_k^\dagger A_k = 1$. We focus here on systems of n qubits so that $D = 2^n$.

We start by expanding the noise operators in a basis of Pauli operators $P_i \in \mathcal{P}_n$ consists of n-fold tensor product of the usual single-qubit Pauli operators $\{1, X, Y, Z\}$, giving $A_k = \sum_{i=1}^{D^2} \alpha_i^{(k)} P_i/\sqrt{D}$, where $\alpha_i^{(k)} = \mathrm{Tr}[A_k P_i]/\sqrt{D}$, and the Pauli's satisfy the orthogonality relation $\mathrm{Tr}[P_i P_j] = D\delta_{ij}$. The Clifford group $\mathcal{C}_n$ is defined as the normalizer of the Pauli group $\mathcal{P}_n$: it consists of all elements U_i of the unitary group $U(D)$ satisfying $U_i P_j U_i^\dagger \in \mathcal{P}_n$ for every $P_j \in \mathcal{P}_n$. For further details of the Clifford group see [5].

We can analyze the effect of the twirl $\mathcal{C}_1^{\otimes n}$ by noting that any element $C_i \in \mathcal{C}_1^{\otimes n}$ can be expressed as $C_i = P_j Y_l$, where $P_j \in \mathcal{P}_n$ and $Y_l \in \mathcal{Y}_1^{\otimes n}$, and where we consider as equivalent elements of each group that differ only by a phase.

Hence, the $\mathcal{C}_1^{\otimes n}$-twirl of an arbitrary channel Λ consists of the action

$$\Lambda(\rho) \to \overline{\Lambda(\rho)} = \frac{1}{|\mathcal{C}_1^{\otimes n}|} \sum_{j=1}^{|\mathcal{S}_1^{\otimes n}|} \sum_{l=1}^{|\mathcal{P}_n|} \sum_k S_j^\dagger P_l^\dagger A_k P_l S_j \rho S_j^\dagger P_l^\dagger A_k^\dagger P_l S_j. \tag{1}$$

where $|\mathcal{C}_1^{\otimes n}| = |\mathcal{S}_1^{\otimes n}|\,|\mathcal{P}_n|$. The effect of the Pauli-twirl is to create the channel $\sum_i a_i P_i \rho P_i$, where $a_i = \sum_k |\alpha_i^{(k)}|^2/D$ are probabilities, known as a Pauli channel. The effect of the symplectic-twirl on the Pauli channel is to map each of the non-identity Pauli operators to a uniform sum over the 3 non-identity Pauli operators. To express this we separate out terms according to their Pauli weight w, where $w \in \{0, \ldots, n\}$ is the number of non-identity factors in P_l. We let the index $\nu_w \in \{1, \ldots, \binom{n}{w}\}$ count the number of distinct ways that w non-identity Pauli operators can be distributed over the n factor spaces, and the index $\mathbf{i}_w = \{i_1, \ldots, i_w\}$ with $i_j \in \{1, 2, 3\}$ denote which of the non-identity Pauli operators occupies the j'th occupied site. Hence we have,

$$\overline{\Lambda(\rho)} = \frac{1}{|\mathcal{S}_1^{\otimes n}|} \sum_{j=1}^{|\mathcal{S}_1^{\otimes n}|} \sum_{w=0}^{n} \sum_{\nu_w=1}^{\binom{n}{w}} \sum_{\mathbf{i}_w=1}^{3^w} a_{w,\nu_w,\mathbf{i}_w} S_j^\dagger P_{w,\nu_w,\mathbf{i}_w} S_j \rho S_j^\dagger P_{w,\nu_w,\mathbf{i}_w} S_j. \tag{2}$$

For any term with arbitrary but fixed w and ν_w the effect of symplectic-twirl is

$$\frac{1}{|\mathcal{S}_1^{\otimes n}|} \sum_{\mathbf{i}_w=1}^{3^w} a_{w,\nu_w,\mathbf{i}_w} \sum_{j=1}^{|\mathcal{S}_1^{\otimes n}|} S_j^\dagger P_{w,\nu_w,\mathbf{i}_w} S_j \rho S_j^\dagger P_{w,\nu_w,\mathbf{i}_w} S_j = \left(\frac{1}{3^w} \sum_{\mathbf{i}_w}^{3^w} a_{w,\nu_w,\mathbf{i}_w} \right) \sum_{\mathbf{j}_w=1}^{3^w} P_{w,\nu_w,\mathbf{j}_w} \rho P_{w,\nu_w,\mathbf{j}_w}. \tag{3}$$

Consequently we obtain,

$$\overline{\Lambda(\rho)} = \sum_{w=0}^{n} \sum_{\nu_w=1}^{\binom{n}{w}} r_{w,\nu_w} \sum_{\mathbf{i}_w=1}^{3^w} P_{w,\nu_w,\mathbf{i}_w} \rho P_{w,\nu_w,\mathbf{i}_w} \tag{4}$$

where $r_{w,\nu_w} = \frac{1}{3^w} \sum_{\mathbf{i}_w=1}^{3^w} a_{w,\nu_w,\mathbf{i}_w}$.

The effect of actual or virtual permutations of the qubits chosen uniformly at random is to produce the effective channel

$$\overline{\Lambda}^{\Pi}(\rho) = \sum_{w=0}^{n} p_w \sum_{\nu_w=1}^{\binom{n}{w}} \sum_{\mathbf{i}_w=1}^{3^w} \frac{1}{3^w \binom{n}{w}} P_{w,\nu_w,\mathbf{i}_w} \rho P_{w,\nu_w,\mathbf{i}_w}, \tag{5}$$

where

$$p_w = 3^w \sum_{\nu_w=1}^{\binom{n}{w}} r_{w,\nu_w}. \tag{6}$$

This symmetrized channel can now be probed experimentally by inputting the initial state $|0\rangle \equiv |0\rangle^{\otimes n}$ and performing a projective measurement in the computational basis $|l\rangle$, where $l \in \{0,1\}^n$. If we distinguish outcome bit strings only according to their Hamming weight $h \in 0, \ldots, n$, the effect is equivalent to a random permutation of the qubits. Observe that only Pauli X and Y errors will affect the Hamming weight because Pauli Z errors commute with the input state. Hence the probability of measuring an outcome with Hamming weight h is

$$u_h = \sum_{w=0}^{n} R_{hw} p_w$$

where $R_{hw} = \binom{w}{h} 2^h/3^w$ gives the number of Pauli operators of weight w of which exactly h are either X or Y, and where

$$p_w = 3^w \sum_{\nu_w=1}^{\binom{n}{w}} r_{w,\nu_w} = \sum_{\nu_w=1}^{\binom{n}{w}} \sum_{\mathbf{i}_w}^{3^w} p_{w,\nu_w,\mathbf{i}_w} \tag{7}$$

is a quantity of interest, i.e., the total probability of all Pauli errors with weight w. Noting that the $n \times n$ matrix R_{hw} satisfies $R_{hw} = 0$ when $h > w$ and hence is upper triangular, estimates of the p_w can be recovered trivially from the measured probabilities u_h after n back-substitutions.

Furthermore, we can determine more direct information about the noise map if we instead distinguish outcome bit strings only by the parity of a random subset of w qubits. The effect of this is also equivalent to a random permutation of the qubits. Thus, we experimentally implement the $\mathcal{C}_1^{\otimes n}$-twirl $\overline{\Lambda(\rho)}$, and virtually implement the permutation-twirl $\overline{\Lambda}^{\Pi}(\rho)$ by averaging over random choices of subsets of w qubits. The probability q_w that the parity of random subset of w qubits is even is related to $\langle\overline{Z^{\otimes w}}\rangle$, the average of all permutations of Pauli operators with w factors of Z and $n - w$ identity factors, according to

$$c_w \equiv \langle\overline{Z^{\otimes w}}\rangle = q_w - (1 - q_w) = 2q_w - 1, \tag{8}$$

where the c_w correspond to the eigenvalues of the twirled map. In order to clarify the information content of the c_w and their relation to the error probabilities p_w we will make use of the Liouville representation of the twirled channel which is described in the following subsection.

Liouville Representation of the Twirled Channel

Because any two operators $P_{m,\nu_m,\mathbf{i}_m} \in \mathcal{P}_n$ either commute or anti-commute, it follows that

$$\overline{\Lambda}^{\Pi}\left(P_{m,\nu_m,\mathbf{i}_m}\right) = \left(\Pr(\text{comm}) - \Pr(\text{anti-comm})\right) P_{m,\nu_m,\mathbf{i}_m} = c_m P_{m,\nu_m,\mathbf{i}_m}, \tag{9}$$

where Pr(comm) (Pr(anti-comm)) is the probability of the channel $\overline{\Lambda}^{\Pi}$ acting with a noise operators $P_{w,\nu_w,\mathbf{i}_w}$ which commutes (anti-commutes) with $P_{m,\nu_m,\mathbf{i}_m}$. Thus, the Pauli operators $P_{m,\nu_m,\mathbf{i}_m}$ are the eigenoperators of the channel with corresponding eigenvalues c_m. The eigendecomposition of $\overline{\Lambda}^{\Pi}$ is given by

$$\overline{\Lambda}^{\Pi}(\rho) = \sum_{w=0}^{n} c_w M_w^c(\rho), \tag{10}$$

where M_w^c are the superoperators

$$M_w^c(\rho) = \frac{1}{2^n} \sum_{\nu_w=0}^{\binom{n}{w}} \sum_{\mathbf{i}_w=0}^{3^w} P_{w,\nu_w,\mathbf{i}_w} \operatorname{tr}(P_{w,\nu_w,\mathbf{i}_w}\rho). \tag{11}$$

We can also rewrite the usual parameterisation of $\overline{\Lambda}^{\Pi}$ as

$$\overline{\Lambda}^{\Pi}(\rho) = \sum_{w=0}^{n} p_w M_w^p(\rho), \tag{12}$$

where M_w^p are the superoperators

$$M_w^p(\rho) = \frac{1}{3^w\binom{n}{w}} \sum_{\nu_w=0}^{\binom{n}{w}} \sum_{\mathbf{i}_w=0}^{3^w} P_{w,\nu_w,\mathbf{i}_w} \rho P_{w,\nu_w,\mathbf{i}_w}. \tag{13}$$

By considering the Liouville representation of these superoperators it is easy to show that the M_w^c are orthogonal and that the M_w^p are orthogonal. Thus, $\{c_w\}_{w=0}^n$ parameterizes the channel $\overline{\Lambda}^{\Pi}$ uniquely, and $\{p_w\}_{w=0}^n$ also parameterizes the same channel uniquely. Using the Liouville representation it follows that these parameterizations are related by a $(n+1) \times (n+1)$ matrix Ω such that

$$c_w = \sum_{w'=0}^{n} p_{w'} \Omega_{w,w'}, \tag{14}$$

$$p_w = \sum_{w'=0}^{n} c_{w'} \Omega^{-1}_{w,w'} \tag{15}$$

with Ω defined by

$$\Omega_{w,w'} = \frac{4^n}{3^{w+w'}\binom{n}{w}\binom{n}{w'}}\langle M_w^c, M_{w'}^p\rangle \tag{16}$$

$$\Omega^{-1}_{w,w'} = \langle M_w^p, M_{w'}^c\rangle, \tag{17}$$

where $\langle\cdot,\cdot\rangle$ is the Hilbert-Schmidt inner product of superoperators acting on Liouville space defining the notion of orthogonality discussed above. To obtain an explicit expression for $\Omega_{w,w'}$, we start from (9) and observe that a Pauli operator of weight w is scaled by a channel of the form

$$\mathcal{N}_{w'}(\rho) = \frac{1}{3^{w'}\binom{n}{w'}}\sum_{\nu_{w'}=0}^{\binom{n}{w'}}\sum_{\mathbf{i}_{w'}=0}^{3^{w'}} P_{w',\nu_{w'},\mathbf{i}_{w'}}\rho P_{w',\nu_{w'},\mathbf{i}_{w'}}. \tag{18}$$

This implies

$$\Omega_{m,w} = -1 + \sum_{L=\max(0,w+m-n)}^{\min(m,w)} \frac{\binom{n-m}{w-L}\binom{m}{L}}{\binom{n}{w}}\frac{3^L+(-1)^L}{3^L}, \tag{19}$$

and, using (16) and (17), it follows that

$$\Omega^{-1}_{m,w} = \frac{3^{m+w}\binom{n}{m}\binom{n}{w}}{4^n}\Omega_{m,w}. \tag{20}$$

For the case of two-qubit channels, this matrix is given by

$$\Omega = \begin{pmatrix} 1 & 1 & 1 \\ 1 & \frac{1}{3} & -\frac{1}{3} \\ 1 & -\frac{1}{3} & \frac{1}{9} \end{pmatrix} \tag{21}$$

$$\Omega^{-1} = \frac{1}{16}\begin{pmatrix} 1 & 6 & 9 \\ 6 & 12 & -18 \\ 9 & -18 & 9 \end{pmatrix}, \tag{22}$$

and for the case of three-qubit channels, it is given by

$$\Omega = \begin{pmatrix} 1 & 1 & 1 & 1 \\ 1 & \frac{5}{9} & \frac{1}{9} & -\frac{1}{3} \\ 1 & \frac{1}{9} & -\frac{5}{27} & \frac{1}{9} \\ 1 & -\frac{1}{3} & \frac{1}{9} & -\frac{1}{27} \end{pmatrix} \tag{23}$$

$$\Omega^{-1} = \frac{1}{64}\begin{pmatrix} 1 & 9 & 27 & 27 \\ 9 & 45 & 27 & -81 \\ 27 & 27 & -135 & 81 \\ 27 & -81 & 81 & -27 \end{pmatrix} \tag{24}$$

Uncorrelated Noise Locations

A noise channel over n qubits that has a distribution of error locations which is uncorrelated, but otherwise arbitrary, is mapped under twirling and random permutations to a channel which is a tensor product of n single-qubit depolarizing channels. Each of these single-qubit channels has the form

$$\mathcal{D}(\rho) = (1-p)\rho + \frac{p}{3}(X\rho X + Y\rho Y + Z\rho Z) \tag{25}$$

and scales a single-qubit Pauli operator by $c_1 = 1 - \frac{4}{3}p$. Thus, the n qubit channel will scale a Pauli operator with weight w by $c_w = c_1^w$.

This is only a necessary condition for the independence of the distribution of error locations because there are correlated error models which can also give rise to this exponential scaling law. Hence, statistical disagreement with the exponential scaling law implies that the distribution of the error locations is (statistically unlikely) to be uncorrelated, although statistical agreement with the scaling law does not guarantee that the errors are uncorrelated.

Circuit Complexity and Statistical Analysis

The circuit complexity is depth 2 with only $2n$ single-qubit gates required for the protocol. The outcome from any single experiment is just a binary string. The number of such trials required to estimate the probability q_w of even parity for a random subset of w bits to within a given precision δ is clearly independent of the number of qubits because the problem is reduced to the simple task of estimating the probability of a 2-outcome classical statistical test. More precisely from the Chernoff inequality, any estimate of the exact average $\mathbb{E}[X] = q_w$ after K *independent trials* satisfies,

$$\Pr(|\frac{1}{K}\sum_{i=1}^{K} X_i - \mathbb{E}[X]| > \delta) \leq 2\exp(-\delta^2 K). \tag{26}$$

We see that the number of experiments required to estimate q_w to precision δ with constant probability is at most,

$$K = \log(2)\delta^{-2},$$

where each experiment is an *independent trial* consisting of a single shot experiment in which the Clifford gates are chosen uniformly at random. The number of experimental trials required to estimate the complete set of probabilities $\{q_1, \ldots, q_w, \ldots q_n\}$ can be obtained from the union bound,

$$\Pr(\cup_w \mathcal{E}_w) \leq \sum_w \Pr(\mathcal{E}_w) \tag{27}$$

which applies for arbitrary events $\mathcal{E}_w$. In our case each $\mathcal{E}_w$ is associated with the event that $|\frac{1}{K}\sum_{k=1}^{K} X_k - \mathbb{E}[X]| > \delta$ and similarly $\cup_w \mathcal{E}_w$ is the probability that at least one of the n estimated probabilities q_w satisfies this property (i.e., is an unacceptable estimate) after K trials. Whence, the probability that at least one of the n estimated probabilities is outside precision δ of the exact probability is bounded above by,

$$\Pr(\cup_w \mathcal{E}_w) \leq 2n\exp(-\delta^2 K).$$

This implies that at most $K = \mathcal{O}(\delta^{-2}\log(2n))$ experimental trials are required to estimate each of the components of the (probability) vector $(q_1, \ldots, q_n)$ to within precision δ with constant probability.

Similarly, for the ensemble QIP scheme, in which n distinct input states must be prepared, the protocol requires $k = \mathcal{O}(\log(2n)/\delta^2)$ runs for each input state in order to estimate the n output parameters c_w to precision δ with constant probability.

Statistical Uncertainty for the p_w Estimates

Given an estimate of the $c_w = \langle Z^{\otimes w}\rangle$ with some variance σ^2, the variance of the estimate of a particular p_w is given by

$$\sigma_w^2 = \sum_{i=0}^{n}\sum_{j=0}^{n} \Omega_{w,i}^{-1}\Omega_{w,j}^{-1}\mathrm{Cov}(c_i, c_j) \tag{28}$$

Assuming the estimates for all c_w have the same variance, the positivity constraint on the covariance matrix of the c_w estimates requires that $|\mathrm{Cov}(c_i, c_j)| \leq \sigma^2$, yielding the upper bound

$$\sigma_w^2 \leq \sigma^2 \sum_i \sum_j \left|\Omega_{w,i}^{-1}\Omega_{w,j}^{-1}\right|. \tag{29}$$

From (9), it is clear that

$$|\Omega_{w,w'}| \leq 1, \tag{30}$$

so the from (20) we have

$$\sigma_w \leq \sigma 3^w \binom{n}{w}. \tag{31}$$

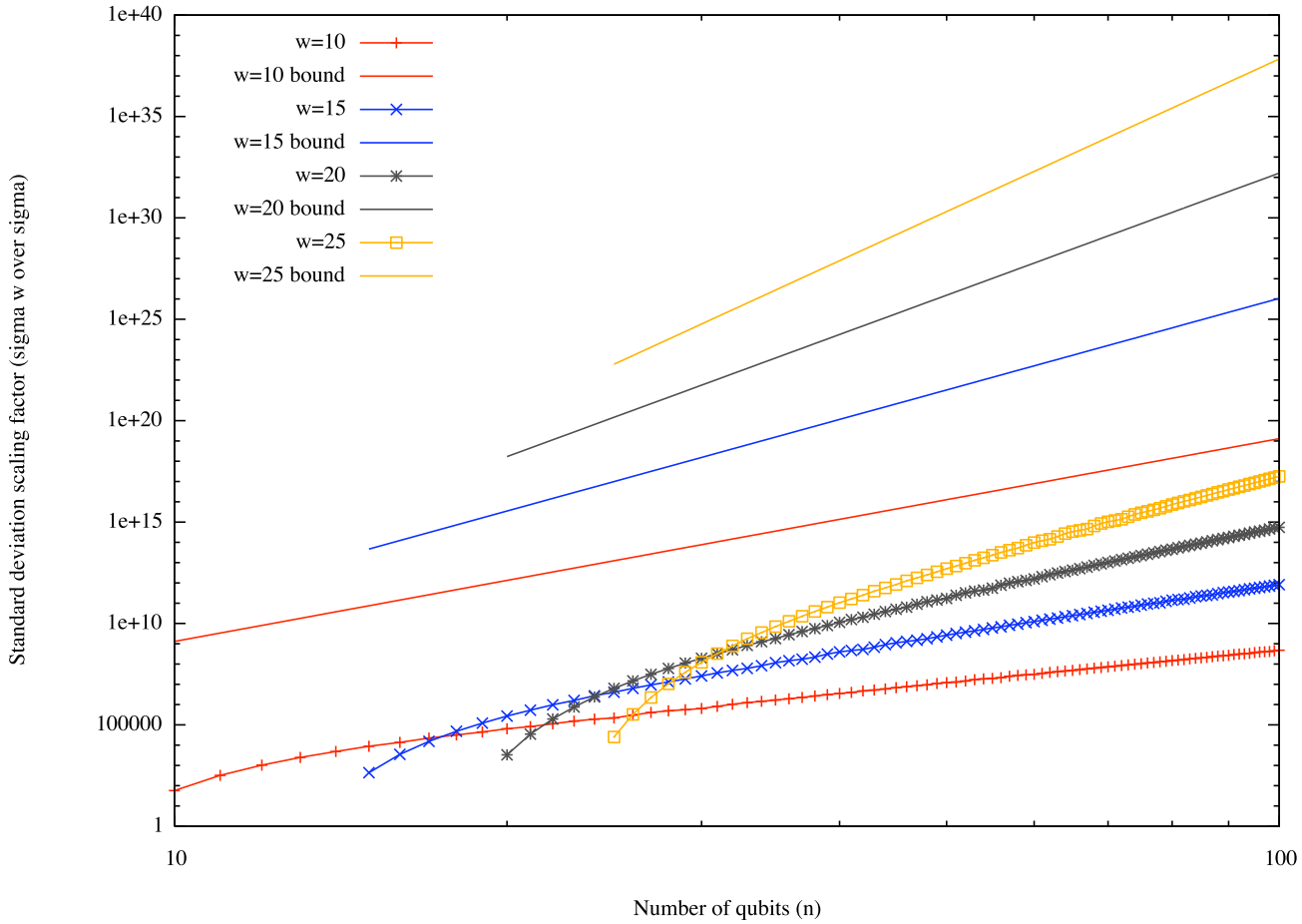

FIG. 2: **Bounds on Standard Deviation for Statistical Estimates of p_w.** Analytic upper bound on standard deviation scaling factor, and numerical calculations for scaling factor with worst case correlations.

Using the fact that

$$\binom{n}{w} \leq \frac{n^w \mathrm{e}^w}{w^w}, \tag{32}$$

we can rigorously show that the uncertainty σ_w on the estimate of p_w is bounded by

$$\sigma_w \leq \sigma \left(\frac{3}{w}\right)^w n^w \mathrm{e}^w. \tag{33}$$

Exact numerical computation of the uncertainty scaling factor $\frac{\sigma_w}{\sigma}$, depicted in Fig. S2, indicates that for fixed w the uncertainty grows as a polynomial in n, but the degree of that polynomial depends linearly on w. For large n, we find that

$$\frac{\sigma_w}{\sigma} \approx \mathrm{e}^{kw+a} n^{mw+b}, \tag{34}$$

where $k = -1.6 \pm 0.1$, $a = 11.8 \pm 1.8$, $m = 0.639 \pm 0.009$, and $b = -0.98 \pm 0.16$.

These numerical results support our analytic bound indicating that applying the c_w estimates to estimate the multi-body noise probabilities p'_w to within a fixed precision, for $0 \leq w' \leq b < n$ with b a constant, requires $O(n^b)$ experiments.

Generalization: the Pauli-twirl

We expect that the $\mathcal{C}_1^{\otimes n}$-twirl is a first step in a hierarchy of tests available under the general symmetrization approach, with each test giving more fine-grained information. One obvious example of a more fine-grained test is a variation of the protocol in which only a Pauli-twirl is applied enables a estimation of the $\mathcal{O}(n^3)$ relative probabilities of Pauli X, Y and Z errors. The full scope of information that can be estimated efficiently via the symmetrisation approach is an important topic for further research.

Solid-state NMR Experimental Results

The results of the solid-state experiments are calculated after factoring out the effect of decoherence occurring during the twirling operations, as described in the main text, in order to isolate the noise associated with the time-suspension sequence. It should be noted that this was a small effect: the twirling operations accounted for only $\simeq 1\%$ fidelity loss per gate.

As noted in the main text, shorter pulse-spacing should lead to improved performance unless there is a competing process at the faster time-scale. Although we see improved performance in the averaging of the homonuclear dipolar Hamiltonian (as evident from experiments #5 and #6 in Table 1), the performance falls short of that expected from numerical simulations of the homonuclear 3-qubit system. In particular, the 5μs pulse-sequence is still limited by decoherence from incomplete (heteronuclear) decoupling of the qubits (carbon nuclei) from the environment (nearby hydrogen nuclei). At the 5μs pulse-spacing the carbon nuclei are being modulated on a time-scale close to the proton decoupling frequency, suggesting that the decoupling sequence may no longer be averaging the heteronuclear coupling to zero. The simple modification of the twirling protocol (in which the permutations are not performed on the weight $w = 1$ input states) allows for determining which qubit accrues the greatest single-qubit errors. The results were consistent with identifying the primary source of single-qubit errors as the qubit whose (heteronuclear) coupling to the hydrogen is an order of magnitude larger than that of the other two qubits.

We have applied the test for the presence of correlations to the experimental results for the c_w from experiments #5 and #6 in Table 1. The results are shown in Fig. S3. For both experiments the results are statistically consistent with the uncorrelated scaling law, though, as already noted, this does not imply that the un-twirled noise consists of uncorrelated errors.

Supporting References and Notes

[1] E. Knill *et al.*, *Nature* **404**, 368 (2000).
[2] J. Baugh *et al.*, *Phys. Rev. A* **73**, 022305 (2006).
[3] B.M. Fung, A.K. Khitrin, K. Ermolaev, *Journal of Magnetic Resonance* **142**, 97 (2000).
[4] N. Khaneja, T. Reiss, C. Kehlet, T.S. Herbruggen, S.J. Glaser, *Journal of Magnetic Resonance* **172**, 296 (2005).
[5] D. Gottesman, Ph.D. Thesis, quant-ph/9705052 (1997).

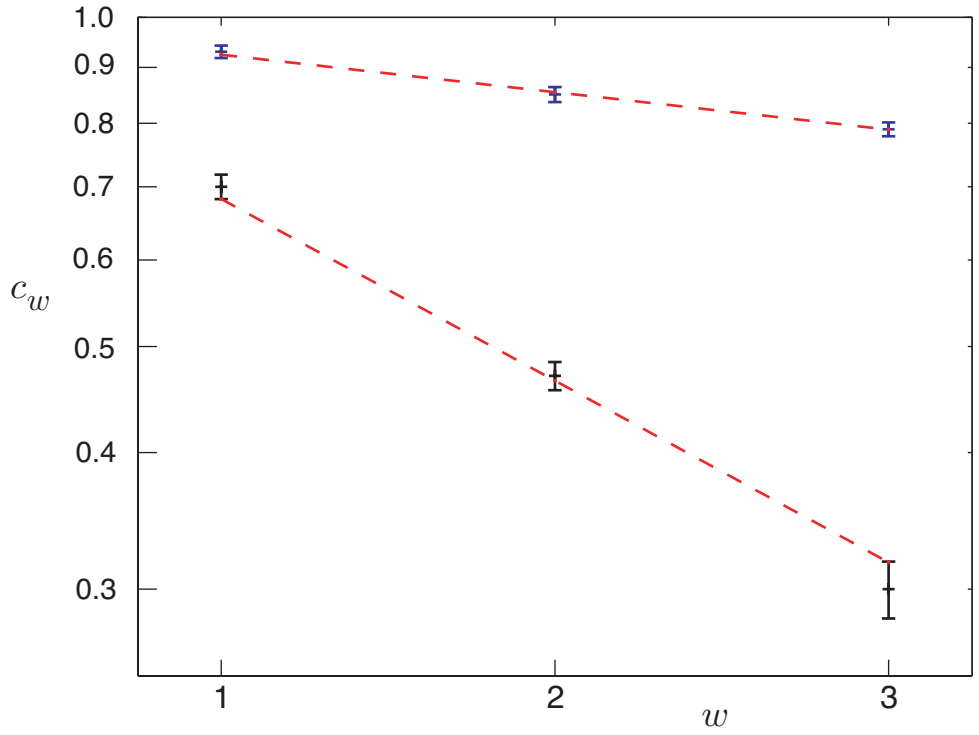

FIG. 3: **Test for Correlations in the Solid-state Experiments.** Experimental values for the c_w for the 5μs (blue) and 10μs (black) pulse-sequences, plotted against the uncorrelated scaling law obtained by a least-squares fit (dashed red) with c_1 as free parameter. Error-bars correspond to statistical (standard deviation) and experimental errors added in quadrature. The goodness-of-fit for the 5μs and 10μs pulse-spacing sequences is $\chi^2 = 0.32$ and $\chi^2 = 1.98$, respectively, for $n_d = 2$.